

## A Numerical Method on Eulerian Grids for Two-Phase Compressible Flow

Yonghui Guo<sup>1</sup>, Ruo Li<sup>2,\*</sup> and Chengbao Yao<sup>3</sup>

<sup>1</sup> Northwest Institute of Nuclear Technology, Xi'an 710024, China

<sup>2</sup> HEDPS & CAPT, LMAM & School of Mathematical Sciences, Peking University, Beijing 100871, China

<sup>3</sup> School of Mathematical Sciences, Peking University, Beijing 100871, and Northwest Institute of Nuclear Technology, Xi'an 710024, China

Received 29 July 2014; Accepted (in revised version) 20 January 2015

---

**Abstract.** We develop a numerical method to simulate a two-phase compressible flow with sharp phase interface on Eulerian grids. The scheme makes use of a levelset to depict the phase interface numerically. The overall scheme is basically a finite volume scheme. By approximately solving a two-phase Riemann problem on the phase interface, the normal phase interface velocity and the pressure are obtained, which is used to update the phase interface and calculate the numerical flux between the flows of two different phases. We adopt an aggregation algorithm to build cell patches around the phase interface to remove the numerical instability due to the breakdown of the CFL constraint by the cell fragments given by the phase interface depicted using the levelset function. The proposed scheme can handle problems with tangential slipping on the phase interface, topological change of the phase interface and extreme contrast in material parameters in a natural way. Though the perfect conservation of the mass, momentum and energy in global is not achieved, it can be quantitatively identified in what extent the global conservation is spoiled. Some numerical examples are presented to validate the numerical method developed.

**AMS subject classifications:** 65M10, 78A48

**Key words:** Two-phase flow, levelset, Riemann problem.

---

## 1 Introduction

Many problems in nature and engineering involve multiphase flows where the flows in different phases are depicted by an immiscible model. Numerical methods to accurately track/capture the interface between two fluids have been an area of research for decades.

---

\*Corresponding author.

Email: gyh661012@163.com (Y. H. Guo), rli@math.pku.edu.cn (R. Li), yaocheng@pku.edu.cn (C. B. Yao)

Tryggvason et al. [17] provided a detailed review on various methods used for direct simulation of multiphase flows. Broadly, these schemes can be classified into two categories: (a) Lagrangian and (b) Eulerian approach.

Lagrangian methods use marker-points connected to each other representing the phase interface, which is tracked by advecting the marker points. In one class of Lagrangian methods [1, 11, 18], the governing equations of the flow are solved on a fixed grid in an Eulerian frame. In another class of Lagrangian methods, the interface is represented by Lagrangian points and the flow field is also evaluated on these points, such as moving particle-methods [5], vortex in cell methods [6, 12], and smoothed-particle hydrodynamics [7]. Pure Lagrangian methods are promising as they avoid enormous memory requirements for a three-dimensional mesh. Some of these methods automatically provide adaptive resolution in the high-curvature region [6] and have been applied successfully to many two-phase flow problems [4, 19, 20]. Although the accuracy of these method is promising, the topological change of the phase interface is not handled automatically, resulting in increased complexity of the algorithm for three-dimensional reconstruction of the interface from marker-points [17], high cost of finding nearest neighbors in the zone of influence of a Lagrangian point, true enforcement of continuity (or incompressibility) conditions, and problems associated with accurate one-sided interpolations near boundaries [6].

Eulerian approaches such as the volume-of-fluid (VOF) [8, 13] or the levelset method [9, 14, 16] are used extensively for two-phase flow computations, which are straightforward in implementation. In the simulation of incompressible flows, the levelset approach is criticized since it does not preserve the volume of the fluids. The VOF formulation, on the other hand, conserves the fluid volume but lacks in the sharpness of the interface. Several improvements to these methods involve combination of the two [15], and particle-levelsets [3] to improve the accuracy.

The method to be developed in this paper is a certain combination of the front tracking method and the levelset method. We use levelset function to represent the phase interface, which is advected by its normal velocity. To calculate the exchange of the flux between two fluids due to the interaction of the fluids on the phase interface and its displacement, we are tracking the characteristic lines of the flow particles. Interior to the bulk of both fluids, the traditional conservative finite volume method is adopted. The evolving of the phase interface is following the standard approach of the levelset method. This makes us concentrate on the calculation of the interface flux. By studying the one dimensional two-phase Riemann problem, we derive an approximated flux contributed at the phase interface, including the terms both from the phase interface movement and the mass interaction. Using this approximated flux, we take the tracking along the characteristic line as a one dimensional problem locally. An aggregation algorithm is adopted to build cell patches around the phase interface so that the CFL constraint can be satisfied even some of the cells in the mesh are cut into smaller fragments by the phase interface. Numerical examples are presented to validate our numerical methods.

The rest of this paper is arranged as follows. In Section 2, the model of the two-

phase flow governed by the Euler equations is introduced. In Section 3, we study the one dimensional case to derive an approximated flux contributed by the phase interface. The numerical scheme is detailed in Section 4 and the numerical examples are given in Section 5.

## 2 Governing equations

Let us consider a two-phase compressible flow in a two/three dimensional domain  $\Omega$ . We are assuming that for any  $t \geq 0$ , the domain  $\Omega$  is divided into two sub-domains  $\Omega^-(t)$  and  $\Omega^+(t)$

$$\overline{\Omega^-(t)} \cup \overline{\Omega^+(t)} = \bar{\Omega}, \quad \overline{\Omega^-(t)} \cap \overline{\Omega^+(t)} = \Gamma^{\text{in}}(t),$$

where  $\Gamma^{\text{in}}(t)$  is the sharp interface between the fluids of two different phases, referred as phase 0 and phase 1, which are immiscible. We denote the state of the fluid by density  $\rho$ , velocity  $\mathbf{u}$  and pressure  $p$ , and the flow variables are governed by the compressible Euler equations

$$\frac{\partial \mathbf{U}}{\partial t} + \nabla \cdot \mathbf{F}(\mathbf{U}) = 0,$$

where

$$\mathbf{U} = \begin{bmatrix} \rho \\ \rho \mathbf{u}^T \\ E \end{bmatrix}, \quad \mathbf{F}(\mathbf{U}) = \begin{bmatrix} \rho \mathbf{u} \\ \rho \mathbf{u} \otimes \mathbf{u} + p \mathbf{I} \\ (E + p) \mathbf{u} \end{bmatrix},$$

and the relation of the total energy  $E$  per unit volume to the other flow variables is given as the equation of state for ideal gas

$$E = \frac{\rho \|\mathbf{u}\|^2}{2} + \frac{p}{\gamma - 1},$$

where the polytropic index  $\gamma$  satisfies the convection equation

$$\frac{\partial \gamma}{\partial t} + \tilde{\mathbf{u}} \cdot \nabla \gamma = 0, \quad (2.1)$$

with interface velocity  $\tilde{\mathbf{u}}$  which is clarified later on. The initial value is given as

$$\mathbf{U}(\mathbf{x}, t=0) = \mathbf{U}_0(\mathbf{x}), \quad \gamma(\mathbf{x}, t=0) = \begin{cases} \gamma_0, & \mathbf{x} \in \Omega^-(t=0), \\ \gamma_1, & \mathbf{x} \in \Omega^+(t=0), \end{cases}$$

where  $\gamma_0$  and  $\gamma_1$  are two constants for the fluids of two different phases. Here we omit the discussion of the boundary condition on  $\partial\Omega$ .

Due to (2.1), the domain interface  $\Gamma^{\text{in}}$  is convected by the interface velocity  $\tilde{u}$ , and the solution of  $\gamma$  is always as

$$\gamma(\mathbf{x}, t) = \begin{cases} \gamma_0, & \mathbf{x} \in \Omega^-(t), \\ \gamma_1, & \mathbf{x} \in \Omega^+(t). \end{cases}$$

Since  $\gamma$  is constant in both sub-domains  $\Omega_i(t)$ ,  $i=0,1$ , it is clear that the value of  $\tilde{u}$  interior of the sub-domains is irrelevant to the evolving of  $\gamma$  in time. This makes one consider the value of  $\tilde{u}$  on the phase interface  $\Gamma^{\text{in}}(t)$  only. Since the fluid velocity may not be a single-valued function on the phase interface  $\Gamma^{\text{in}}(t)$  due to the discontinuity of the solution, the convective velocity  $\tilde{u}$  of  $\gamma$  in (2.1) can not be simply assigned as  $\mathbf{u}$ . For a point  $\mathbf{x}$  on the phase interface  $\Gamma^{\text{in}}(t)$ , we denote the unit normal of  $\Gamma^{\text{in}}(t)$  at  $\mathbf{x}$  as  $\mathbf{n}(\mathbf{x}, t)$  pointing to the interior of  $\Omega^+(t)$ . The conservative variables of the fluids on both side of  $\Gamma^{\text{in}}(t)$  at  $\mathbf{x}$  are denoted as

$$\mathbf{U}^- = [\rho^-, \rho^- \mathbf{u}^- \cdot \mathbf{n}, E^-]^T, \quad [\rho^-, \rho^- \mathbf{u}^-, E^-]^T = \lim_{\tau \rightarrow 0} \mathbf{U}(\mathbf{x} - \tau \mathbf{n}, t), \quad (2.2a)$$

$$\mathbf{U}^+ = [\rho^+, \rho^+ \mathbf{u}^+ \cdot \mathbf{n}, E^+]^T, \quad [\rho^+, \rho^+ \mathbf{u}^+, E^+]^T = \lim_{\tau \rightarrow 0} \mathbf{U}(\mathbf{x} + \tau \mathbf{n}, t). \quad (2.2b)$$

We propose a one dimensional Riemann problem

$$\frac{\partial}{\partial t} \begin{bmatrix} \rho \\ \rho u \\ E \end{bmatrix} + \frac{\partial}{\partial x} \begin{bmatrix} \rho u \\ \rho u^2 + p \\ (E + p)u \end{bmatrix} = 0, \quad (2.3a)$$

$$\frac{\partial \gamma}{\partial t} + u \frac{\partial \gamma}{\partial x} = 0, \quad (2.3b)$$

where

$$p = (\gamma - 1)(E - \rho u^2 / 2),$$

$$\begin{bmatrix} \rho \\ \rho u \\ E \\ \gamma \end{bmatrix}_{t=0} = \begin{cases} \begin{bmatrix} \mathbf{U}^- \\ \gamma_0 \end{bmatrix}, & x < 0, \\ \begin{bmatrix} \mathbf{U}^+ \\ \gamma_1 \end{bmatrix}, & x > 0. \end{cases}$$

Due to the conservative structure of the equations, the two-phase Riemann problem admits a self-similar solution as

$$\begin{bmatrix} \rho \\ \rho u \\ E \end{bmatrix} (x, t) = \begin{bmatrix} \rho \\ \rho u \\ E \end{bmatrix} (x/t).$$

Particularly, we are pursuing the self-similar solution that the polytropic index is following the translation of the mass, thus

$$\gamma(x, t) = \gamma(x/t).$$

Since the two fluids are immiscible, the self-similar solution has to equip with a constant velocity  $V(\mathbf{U}^-, \mathbf{U}^+)$  of the phase interface point. The phase interface point is then located on

$$x/t = V(\mathbf{U}^-, \mathbf{U}^+).$$

As the result, the expression of  $\gamma$  following the movement of the mass is

$$\gamma(x, t) = \begin{cases} \gamma_0, & x/t < V(\mathbf{U}^-, \mathbf{U}^+), \\ \gamma_1, & x/t > V(\mathbf{U}^-, \mathbf{U}^+). \end{cases}$$

The phase interface is a contact discontinuity, connecting two constant states  $U_\star^-$  and  $U_\star^+$ , thus the flow velocity across the contact discontinuity is constant. The Rankine-Hugoniot condition then provides us that the pressure is constant across the contact discontinuity, denoted as  $P(\mathbf{U}^-, \mathbf{U}^+)$ .

We then assign the value of  $\tilde{u}$  at  $x$  as

$$\tilde{u}(x, t) = V(\mathbf{U}^-, \mathbf{U}^+)n(x, t).$$

The flux across the contact discontinuity is thus as

$$[0, P(\mathbf{U}^-, \mathbf{U}^+)n(x, t), P(\mathbf{U}^-, \mathbf{U}^+)V(\mathbf{U}^-, \mathbf{U}^+)]^T.$$

**Remark 2.1.** To circumvent even subtle Riemann solution structure, we assume that no cavitation appears in the fluid, particularly on the phase interface  $\Gamma^{\text{in}}$ .

### 3 Interface flux

We consider a one dimensional model to demonstrate how to approximate the flux on the phase interface used in the numerical scheme. Given a sequence of one dimensional grid points  $x_k \in \mathbb{R}$  as

$$x_{-1} < x_0 < \cdots < x_{n-1} < x_n,$$

we try to obtain the approximated flux to every cell in the grid contributed by a Riemann solution from  $t = 0$  up to  $t = T$  in one time step in a numerical style. Precisely, if the knowledge of the whole structure of the Riemann fan is not available<sup>†</sup>, except for the velocity of the phase interface and the pressure there, the flux contributed to the grid points and the phase interface is to be approximated. Without loss of generality, the phase interface at  $t = 0$  is assumed to be  $x_\star \in (x_{-1}, x_0)$  and the phase interface at  $t = T$  is to be  $x^\star \in (x_{n-1}, x_n)$ . As the initial value, we have

$$[\rho, \rho u, E]_{t=0} = \begin{cases} \mathbf{U}^- = [\rho_l, \rho_l u_l, E_l], & x < x_\star, \\ \mathbf{U}^+ = [\rho_r, \rho_r u_r, E_r], & x > x_\star. \end{cases}$$

<sup>†</sup>It is too expansive to have the complete structure of the Riemann fan.

The self-similar Riemannian solution developed from such an initial value may result in a phase interface with velocity  $V = V(\mathbf{U}^-, \mathbf{U}^+) = X/T$ , where  $X = |x^* - x_*|$ , and corresponding pressure on the phase interface  $P = P(\mathbf{U}^-, \mathbf{U}^+)$ . In front and behind of the phase interface, the structure of the Riemannian solution gives a piece of constant area as

$$\begin{aligned}\mathbf{U}^{-,*} &= \left[ \rho_l^*, \rho_l^* V, \frac{1}{2} \rho_l^* V^2 + \frac{P}{\gamma_l - 1} \right], \\ \mathbf{U}^{+,*} &= \left[ \rho_r^*, \rho_r^* V, \frac{1}{2} \rho_r^* V^2 + \frac{P}{\gamma_r - 1} \right],\end{aligned}$$

which is not available without the knowledge of the full structure of the Riemannian solution. For stability based on CFL constraint, we consider the case that  $|x_* - x_{-1}|$  and  $|x_n - x^*|$  are great enough that the Riemann fan is restricted in  $(x_{-1}, x_n)$ .

Let  $t_k = |x_k - x_*|/V$ , for  $k = 1, \dots, n-1$ ,  $t_0 = 0$ ,  $t_n = T$ , and denote  $\delta t_k = t_k - t_{k-1}$ , for  $k = 1, \dots, n$ . Correspondingly, we denote  $\delta x_k = |x_k - x_{k-1}|$ ,  $k = 1, \dots, n-1$ ,  $\delta x_0 = |x_0 - x_*|$  and  $\delta x_n = |x^* - x_{n-1}|$ .

At  $t = 0$ , the flux at  $x_{-1}$  is  $u_l \mathbf{U}^-$  since  $x_{-1}$  is located in the bulk of phase 0 and the flux at  $x_k$ ,  $0 \leq k \leq n-1$ , is  $u_r \mathbf{U}^+$  since  $x_k$  is located in the bulk of phase 1. For  $t > 0$  that  $x_k$ ,  $0 \leq k \leq n-1$ , is located in the constant area vicinity to the phase interface in the Riemannian solution, the flux at the  $x_k$  is as  $V \mathbf{U}^{-,*}$  and  $V \mathbf{U}^{+,*}$  for phase 0 and phase 1, respectively. Since  $\mathbf{U}^{-,*}$  and  $\mathbf{U}^{+,*}$  are not available, the flux at grid point  $x_k$  at any time  $t$  is always approximately taken as  $V \mathbf{U}^-$  if it is located in phase 0 and  $V \mathbf{U}^+$  if it is located in phase 1. Such formula is a mixture of the phase interface velocity and the initial value, which is the data assumed to be available in a reasonable way. The time period is  $|x^* - x_k|/V$  for  $x_k$  located in phase 0, and is  $|x_k - x_*|/V$  for  $x_k$  located in phase 1,  $0 \leq k \leq n-1$ . Then the approximated flux at a point  $x_k$ ,  $0 \leq k \leq n-1$ , is

$$(x^* - x_k) \mathbf{U}^- \quad \text{and} \quad (x_k - x_*) \mathbf{U}^+$$

for phase 0 and phase 1, respectively.

The flux at the phase interface  $(x_* + tV, t)$  is always  $\hat{\mathbf{F}} = [0, P, PV]$ . The time of period that the phase interface is located in the cell  $(x_{k-1}, x_k)$  is then  $\delta t_k$ , thus the flux contributed on  $(x_{k-1}, x_k)$  due to the phase interface is

$$-\delta t_k \hat{\mathbf{F}} \quad \text{and} \quad \delta t_k \hat{\mathbf{F}}, \quad 0 \leq k \leq n,$$

for phase 0 and phase 1, respectively.

Collecting the flux due to the phase interface flux and due to the convection interior to both phases, the contribution of the flux on the cells is obtained as below:

- For phase 0:

- in cell  $(x_{-1}, x_0)$ :

$$\begin{aligned}\hat{\mathbf{F}}_0^- &= -(x^* - x_0)\mathbf{U}^- - \delta t_0 \hat{\mathbf{F}} \\ &= (-X + \delta x_0)\mathbf{U}^- - \delta t_0 \hat{\mathbf{F}} \\ &= (-T + \delta t_0)V\mathbf{U}^- - \delta t_0 \hat{\mathbf{F}}.\end{aligned}$$

- in cell  $(x_{k-1}, x_k)$ ,  $1 < k < n-1$ :

$$\begin{aligned}\hat{\mathbf{F}}_k^- &= (x^* - x_{k-1})\mathbf{U}^- - (x^* - x_k)\mathbf{U}^- - \delta t_k \hat{\mathbf{F}} \\ &= \delta x_k \mathbf{U}^- - \delta t_k \hat{\mathbf{F}} \\ &= \delta t_k V \mathbf{U}^- - \delta t_k \hat{\mathbf{F}}.\end{aligned}$$

- in cell  $(x_{n-1}, x_n)$ :

$$\hat{\mathbf{F}}_n^- = \delta x_n \mathbf{U}^- - \delta t_n \hat{\mathbf{F}} = \delta t_n V \mathbf{U}^- - \delta t_n \hat{\mathbf{F}}.$$

- For phase 1:

- in cell  $(x_{-1}, x_0)$ :

$$\hat{\mathbf{F}}_0^+ = -(x_0 - x_*)\mathbf{U}^+ + \delta t_0 \hat{\mathbf{F}} = -\delta t_0 V \mathbf{U}^+ + \delta t_0 \hat{\mathbf{F}}.$$

- in cell  $(x_{k-1}, x_k)$ ,  $1 < k < n-1$ :

$$\begin{aligned}\hat{\mathbf{F}}_k^+ &= (x_{k-1} - x_*)\mathbf{U}^+ - (x_k - x_*)\mathbf{U}^+ + \delta t_k \hat{\mathbf{F}} \\ &= -\delta x_k \mathbf{U}^+ + \delta t_k \hat{\mathbf{F}} \\ &= -\delta t_k V \mathbf{U}^+ + \delta t_k \hat{\mathbf{F}}.\end{aligned}$$

- in cell  $(x_{n-1}, x_n)$ :

$$\begin{aligned}\hat{\mathbf{F}}_n^+ &= (x_{n-1} - x_*)\mathbf{U}^+ + \delta t_n \hat{\mathbf{F}} \\ &= (X - \delta x_n)\mathbf{U}^+ + \delta t_n \hat{\mathbf{F}} \\ &= (T - \delta t_n)V\mathbf{U}^+ + \delta t_n \hat{\mathbf{F}}.\end{aligned}$$

If we consider the case  $V < 0$  that the phase interface point is travelling left, the similar formula can be derived. Precisely, the above procedure can be carried out on the grid points

$$x_{-1} > x_0 > \cdots > x_{n-1} > x_n$$

to have results with only slight differences. We collect the flux for both cases  $V > 0$  and  $V < 0$  into an unified formulation as

$$\hat{\mathbf{F}}_k^\pm = (\delta_{k,V}^\pm T \mp \delta t_k) V \mathbf{U}^\pm \pm \delta t_k \hat{\mathbf{F}}, \quad 0 \leq k \leq n,$$

where if  $V > 0$ ,

$$\delta_{k,V}^- = \begin{cases} -1, & k=0, \\ 0, & 1 \leq k \leq n, \end{cases} \quad \delta_{k,V}^+ = \begin{cases} 0, & 0 \leq k \leq n-1, \\ +1, & k=n, \end{cases}$$

else if  $V < 0$ ,

$$\delta_{k,V}^- = \begin{cases} 0, & 0 \leq k \leq n-1, \\ -1, & k=n, \end{cases} \quad \delta_{k,V}^+ = \begin{cases} +1, & k=0, \\ 0, & 1 \leq k \leq n. \end{cases}$$

It is clear that

$$\sum_{k=0}^n \hat{\mathbf{F}}_k^\pm = \pm T \hat{\mathbf{F}},$$

and

$$\sum_{k=0}^n \{ \hat{\mathbf{F}}_k^- + \hat{\mathbf{F}}_k^+ \} = 0.$$

**Remark 3.1.** If the structure of the Riemann fan includes only a single contact discontinuity, the flux above is accurate.

## 4 Numerical scheme

We triangulate the domain into a conforming mesh  $\mathcal{T}$  with simplex cells. The cells in the mesh are denoted as  $\tau_i$ , and

$$\bar{\Omega} = \bigcup_{i=1}^N \bar{\tau}_i.$$

The intersection of two different cells is empty set,  $\tau_i \cap \tau_j = \emptyset$  if  $i \neq j$ . For two different cells  $\tau_i$  and  $\tau_j$ , its common boundary

$$s_{ij} = \bar{\tau}_i \cap \bar{\tau}_j$$

is an edge (two dimensional) or a face (three dimensional) in the mesh  $\mathcal{T}$  if  $s \neq \emptyset$ . For two dimensional domain,  $s_{ij}$  is a line segment and for three dimensional domain,  $s_{ij}$  is a triangle. The unit normal of  $s_{ij}$  pointing from  $\tau_i$  to  $\tau_j$  is denoted as  $\mathbf{n}_{ij}$ , thus it is the unit outer normal for  $\tau_i$ .

On the mesh  $\mathcal{T}$ , we define the piecewise constant finite element space

$$W_h^0(\Omega) = \{ w_h \in L^1(\Omega) : w_h|_{\tau_i} \in \mathbb{P}^0(\mathbf{x}) \}$$

and the piecewise linear finite element space

$$W_h^1(\Omega) = \{ w_h \in C^0(\Omega) : w_h|_{\tau_i} \in \mathbb{P}^1(\mathbf{x}) \}.$$



At every time step  $t_n$ , we adopt two sets of flow variables

$$\mathbf{U}_{h,n}^- = \begin{bmatrix} \rho_{h,n}^- \\ (\rho \mathbf{u})_{h,n}^- \\ E_{h,n}^- \end{bmatrix}, \quad \mathbf{U}_{h,n}^+ = \begin{bmatrix} \rho_{h,n}^+ \\ (\rho \mathbf{u})_{h,n}^+ \\ E_{h,n}^+ \end{bmatrix}.$$

Each component of  $\mathbf{U}_{h,n}^-$  and  $\mathbf{U}_{h,n}^+$  is in  $W_h^0(\Omega)$ . In every cell  $\tau$ , the flow variables are constant denoted as  $\mathbf{U}_{\tau,n}^-$  and  $\mathbf{U}_{\tau,n}^+$ . At the same time, we introduce a function  $\phi_{h,n} \in W_h^1(\Omega)$ . The domain  $\Omega$  is divided into two parts

$$\Omega_h^-(t_n) = \{x \in \Omega : \phi_{h,n}(x) < 0\} \quad \text{and} \quad \Omega_h^+(t_n) = \{x \in \Omega : \phi_{h,n}(x) > 0\}.$$

We denote the zero levelset of  $\phi_{h,n}$  as  $\Gamma_{h,n}^{\text{in}}$ . A cell  $\tau$  in the mesh  $\mathcal{T}$  is marked as phase interface cells if  $\Gamma_{\tau,n}^{\text{in}} \neq \emptyset$ , where

$$\Gamma_{\tau,n}^{\text{in}} \triangleq \Gamma_{h,n}^{\text{in}} \cup \bar{\tau}.$$

Since  $\phi_{h,n}$  is piecewise linear and the cell is simplex,  $\Gamma_{\tau,n}^{\text{in}}$  can only be a linear manifold. Precisely,  $\Gamma_{\tau,n}^{\text{in}}$  is a line segment for two dimensional domain and is a triangle or a quadrangle for three dimensional domain.  $\Gamma_{\tau,n}^{\text{in}}$  cuts the cell  $\tau$  into two parts, denoted as

$$\tau_n^\pm = \tau \cup \Omega_h^\pm(t_n).$$

The unit normal of  $\Gamma_{\tau,n}^{\text{in}}$  pointing from  $\tau_n^-$  to  $\tau_n^+$  is denoted as  $\mathbf{n}_{\tau,n}$ . For the common boundary  $s_{ij}$  of cell  $\tau_i$  and cell  $\tau_j$ , the zero levelset of  $\phi_{h,n}$  may divide it into two parts, too. We denoted these two parts as

$$s_{ij,n}^\pm = s_{ij} \cup \Omega_h^\pm(t_n).$$

#### 4.1 Initial value

Let us discuss the discretization of the initial value at first. For  $n=0$  and  $t_0=0$ , we define that

$$\phi(x, t=0) = \begin{cases} -\text{dist}(x, \Gamma^{\text{in}}(t=0)), & x \in \Omega^-(t=0), \\ +\text{dist}(x, \Gamma^{\text{in}}(t=0)), & x \in \Omega^+(t=0), \end{cases}$$

which is the levelset function. It is the signed distance from the point  $x$  to the phase interface at  $t=0$ . The function  $\phi_{h,0}$  is then assigned as the interpolation of  $\phi|_{t=0}$  that for every vertex  $\mathbf{X}_i$  of the cells in the mesh  $\mathcal{T}$ ,

$$\phi_{h,0}(\mathbf{X}_i) = \phi(\mathbf{X}_i, 0), \quad \forall \mathbf{X}_i \in \mathcal{T}.$$

On a cell  $\tau$  in the mesh  $\mathcal{T}$ , the values of the flow variables are set as

$$\begin{aligned} \mathbf{u}_{h,0}^-|_{\tau} &= \frac{1}{|\tau \cup \Omega^-(0)|} \int_{\tau \cup \Omega^-(0)} \mathbf{u}_0(\mathbf{x}) d\mathbf{x}, \\ \mathbf{u}_{h,0}^+|_{\tau} &= \frac{1}{|\tau \cup \Omega^+(0)|} \int_{\tau \cup \Omega^+(0)} \mathbf{u}_0(\mathbf{x}) d\mathbf{x}. \end{aligned}$$

Assume that the numerical solution at time step  $n$ ,  $t = t_n$ , is obtained. In the following, we give the numerical scheme to obtain the numerical solution for time step  $n+1$ . The overall procedure of the scheme in one time step is as below:

**Algorithm 4.1.**

1. Evolving the phase interface to obtain  $\phi_{h,n+1}$ ;
2. Calculate the numerical flux and obtain an intermediate value for  $\mathbf{u}_{h,n+1}^{\pm,*}$ ;
3. Post-process the intermediate solution to get  $\mathbf{u}_{h,n+1}^{\pm}$ ;

## 4.2 The evolving of phase interface

As the first step, we numerically solve the Riemannian problem on the phase interface  $\Gamma_{\tau,n}^{\text{in}}$  in a cell  $\tau$ . Let

$$\mathbf{U}^- = \begin{bmatrix} \rho_{h,n}^-|_{\tau} \\ (\rho \mathbf{u})_{h,n}^-|_{\tau} \cdot \mathbf{n}_{\tau,n} \\ E_{h,n}^-|_{\tau} \end{bmatrix}, \quad \mathbf{U}^+ = \begin{bmatrix} \rho_{h,n}^+|_{\tau} \\ (\rho \mathbf{u})_{h,n}^+|_{\tau} \cdot \mathbf{n}_{\tau,n} \\ E_{h,n}^+|_{\tau} \end{bmatrix}.$$

The Riemannian solver gives us  $V_{\tau,n} = V(\mathbf{U}^-, \mathbf{U}^+)$  and  $P_{\tau,n} = P(\mathbf{U}^-, \mathbf{U}^+)$ . The flux on  $\Gamma_{\tau,n}^{\text{in}}$  is calculated as

$$\hat{\mathbf{F}}_{\Gamma_{\tau,n}^{\text{in}}} = \begin{bmatrix} 0 \\ P_{\tau,n} \mathbf{n}_{\tau,n} \\ P_{\tau,n} V_{\tau,n} \end{bmatrix}.$$

The velocity  $V_{\tau,n}$  given on all phase interface cells provides us a piecewise normal velocity for the phase interface  $\Gamma_{h,n}^{\text{in}}$ . We carry out a certain extension of the normal velocity (such as the harmonic extension following [2]) on  $\Gamma_{h,n}^{\text{in}}$  to obtain a piecewise constant velocity field  $V_{h,n}$  on the whole domain  $\Omega$ , which provides a velocity  $V_{h,\tau}$  on every cell  $\tau$ . For every vertices  $\mathbf{X}_i \in \bar{\tau}$ , the characteristic line tracking gives us a point

$$\mathbf{X}_{i,\tau} = \mathbf{X}_i - (t_{n+1} - t_n) V_{h,\tau}.$$

After that, we obtain  $\phi_{h,n+1}$  by set it as an algebraic average as

$$\phi_{h,n+1}^*(\mathbf{X}_i) = \frac{\sum_{\mathbf{X}_i, \mathbf{X}_{i,\tau} \in \bar{\tau}} \phi_{h,n}(\mathbf{X}_{i,\tau})}{\sum_{\mathbf{X}_i, \mathbf{X}_{i,\tau} \in \bar{\tau}} 1}.$$

The levelset function  $\phi_{h,n+1}$  is then obtained after the reinitialization of  $\phi_{h,n+1}^*$  by numerically solving the Eikonal equation

$$\frac{\partial \phi}{\partial t} + \text{sign}(\phi)|1 - \nabla \phi| = 0.$$

We solve this equation by using an explicitly positive coefficient scheme [2] within a narrow band in our implementation.

### 4.3 Numerical flux

#### 4.3.1 Phase interface flux

For the phase interface  $\Gamma_{\tau,n}^{\text{in}}$  in a cell  $\tau$ , we consider the patch covered by the line segments starting from  $\Gamma_{\tau,n}^{\text{in}}$  and ending at  $\Gamma_{h,n+1}$

$$\delta\Omega_{\tau,n}^{\pm} \triangleq \{x = x_0 + sV_{\tau,n}^{\pm} : x_0 \in \Gamma_{\tau,n}^{\text{in}}, \phi_{h,n}(x)\phi_{h,n+1}(x) \leq 0, s \geq 0\},$$

where

$$V_{\tau,n}^{\pm} = \tau_{\tau,n}^{\pm} + V_{\tau,n}n_{\tau,n},$$

and  $\tau_{\tau,n}^{\pm}$  is the velocity of phase 0/1 in  $\tau$  tangential to  $\Gamma_{\tau,n}^{\text{in}}$

$$\tau_{\tau,n}^{\pm} = u_{\tau,n}^{\pm} - (u_{\tau,n}^{\pm} \cdot n_{\tau,n})n_{\tau,n}.$$

We point out that one may have  $x \notin \tau$  for  $x \in \delta\Omega_{\tau,n}^{\pm}$ . For any  $x_0 \in \Gamma_{\tau,n}^{\text{in}}$ , the constraint  $\phi_{h,n}(x)\phi_{h,n+1}(x) \leq 0$  and  $s \geq 0$  make  $s$  to be in an interval denoted as  $I_{\tau,n,x_0}^{\pm} = [0, s_{x_0}^{\pm}]$ . This interval is divided into a sequence of small intervals by the mesh as

$$I_{\tau,n,x_0}^{\pm} = \begin{array}{ccccccc} I_{\tau,n,x_0}^{\pm,0} & \cup & I_{\tau,n,x_0}^{\pm,1} & \cup & \dots & \cup & I_{\tau,n,x_0}^{\pm,K_{x_0}} \\ \downarrow & & \downarrow & & \downarrow & & \downarrow \\ [s_{x_0}^{\pm,0}, s_{x_0}^{\pm,1}] & & [s_{x_0}^{\pm,1}, s_{x_0}^{\pm,2}] & & \dots & & [s_{x_0}^{\pm,K_{x_0}}, s_{x_0}^{\pm,K_{x_0}+1}] \end{array},$$

where

$$s_{x_0}^{\pm,0} = 0, \quad s_{x_0}^{\pm,k} \leq s_{x_0}^{\pm,k+1}, \quad s_{x_0}^{\pm,K_{x_0}+1} = s_{x_0}^{\pm},$$

and every small interval  $I_{\tau,n,x_0}^{\pm,k}$ ,  $0 \leq k \leq K_{x_0}$ , gives a line segment

$$\{x_0 + sV_{\tau,n}^{\pm} : s \in I_{\tau,n,x_0}^{\pm,k}\},$$

which is in a single cell denoted as  $\tau_{\tau,x_0}^{\pm,k}$ . It is clear that the cell  $\tau_{\tau,x_0}^{\pm,0}$  is  $\tau$ . Based on the analysis of the approximated flux in the structure of a one dimensional Riemann fan in the last section, we denote

$$\hat{F}_{\tau,n,x_0}^{\pm,k} \triangleq (\delta_{k,V_{\tau,n}}^{\pm} |I_{\tau,n,x_0}^{\pm}| \mp |I_{\tau,n,x_0}^{\pm,k}|) V_{\tau,n} u_{\tau,n}^{\pm} \pm \frac{|I_{\tau,n,x_0}^{\pm,k}|}{|I_{\tau,n,x_0}^{\pm}|} \Delta t_n \hat{F}_{\Gamma_{\tau,n}^{\text{in}}}, \quad 0 \leq k \leq K_{x_0},$$

where  $|I_{\tau,n,x_0}^{\pm}| = s_{\tau,n}^{\pm}$ ,  $|I_{\tau,n,x_0}^{\pm,k}| = s_{x_0}^{\pm,k+1} - s_{x_0}^{\pm,k}$ , and if  $V_{\tau,n} > 0$

$$\delta_{k,V_{\tau,n}}^{-} = \begin{cases} -1, & k=0, \\ 0, & 1 \leq k \leq K_{x_0}, \end{cases} \quad \delta_{k,V_{\tau,n}}^{+} = \begin{cases} 0, & 0 \leq k \leq K_{x_0}-1, \\ +1, & k=K_{x_0}, \end{cases}$$

else if  $V_{\tau,n} < 0$

$$\delta_{k,V_{\tau,n}}^{-} = \begin{cases} 0, & 0 \leq k \leq K_{x_0}-1, \\ -1, & k=K_{x_0}, \end{cases} \quad \delta_{k,V_{\tau,n}}^{+} = \begin{cases} +1, & k=0, \\ 0, & 1 \leq k \leq K_{x_0}. \end{cases}$$

By  $\sum_{k=0}^{K_{x_0}} |I_{\tau,n,x_0}^{\pm,k}| = |I_{\tau,n,x_0}^{\pm}|$ , we note that

$$\sum_{k=0}^{K_{x_0}} \hat{F}_{\tau,n,x_0}^{\pm,k} = \pm \Delta t_n \hat{F}_{\tau,n}^{\text{in}}. \quad (4.1)$$

We choose a group of representative points  $\{x_1, x_2, \dots, x_L\}$ ,  $x_l \in \Gamma_{\tau,n}^{\text{in}}$  and corresponding weights  $\{w_1, w_2, \dots, w_L\}$  that  $\sum_{l=1}^L w_l = 1$ . These representative points and corresponding weights give us a numerical quadrature formula on  $\Gamma_{\tau,n}^{\text{in}}$  as

$$\frac{1}{|\Gamma_{\tau,n}^{\text{in}}|} \int_{\Gamma_{\tau,n}^{\text{in}}} f(x) ds \approx \sum_{l=1}^L w_l f(x_l),$$

for any function  $f(x)$  defined over  $\Gamma_{\tau,n}^{\text{in}}$  with certain regularity. The contribution of the numerical flux from the phase interface  $\Gamma_{\tau,n}^{\text{in}}$  to a prescribed cell  $\hat{\tau}$  is approximated by using this numerical quadrature formula to have

$$\hat{F}_{\Gamma_{\tau,n}^{\text{in}} \rightarrow \hat{\tau}}^{\pm} = |\Gamma_{\tau,n}^{\text{in}}| \sum_{l=1}^L w_l \hat{F}_{\tau,n,x_l}^{\pm,k_l}, \quad (4.2)$$

where  $k_l$  is the index that the cell  $\hat{\tau}$  is exactly the cell  $\tau_{\tau,x_l}^{\pm,k_l}$ . Summing the numerical flux in the formation of (4.2) over all the phase interface  $\Gamma_{\tau,n}^{\text{in}}$ , the contribution of the numerical flux to a cell  $\hat{\tau}$  due to this term is approximated by

$$\hat{F}_{\hat{\tau},n}^{\pm} = \sum_{\Gamma_{\tau,n}^{\text{in}} \in \Gamma_{h,n}^{\text{in}}} \hat{F}_{\Gamma_{\tau,n}^{\text{in}} \rightarrow \hat{\tau}}^{\pm}. \quad (4.3)$$

We note that only for those cell  $\hat{\tau}$  that  $\hat{\tau} \cup \delta\Omega_{\tau,n}^{\pm} \neq \emptyset$ , for some  $\Gamma_{\tau,n}^{\text{in}} \in \Gamma_{h,n}^{\text{in}}$ , the term  $\hat{F}_{\hat{\tau},n}^{\pm}$  is not vanished.

#### 4.3.2 Cell boundary flux

On every  $s_{ij,n}^{\pm} \neq \emptyset$ , the flux is calculated as

$$\hat{F}_{ij,n}^{\pm} = \Delta t_n |s_{ij,n}^{\pm}| \hat{F}(\mathbf{u}_{h,n}^{\pm}|_{\tau_i}, \mathbf{u}_{h,n}^{\pm}|_{\tau_j}; \mathbf{n}_{ij}), \quad (4.4)$$

where  $\hat{F}(\mathbf{U}_l, \mathbf{U}_r; \mathbf{n})$  is a consistent monotonic numerical flux along  $\mathbf{n}$ , such as the local Lax-Friedrich flux as

$$\hat{F}(\mathbf{U}_l, \mathbf{U}_r; \mathbf{n}) = \frac{1}{2} (F(\mathbf{U}_l) + F(\mathbf{U}_r)) \cdot \mathbf{n} - \lambda (\mathbf{U}_r - \mathbf{U}_l),$$

where  $\lambda = \max\{\lambda_l, \lambda_r\}$ ,  $\lambda_l$  and  $\lambda_r$  are the maximal signal speeds for  $\mathbf{U}_l$  and  $\mathbf{U}_r$ , respectively.

### 4.3.3 Conservative variables updation

With the fluxes (4.3) and (4.4) given, the integration of the flow variables on a cell  $\tau_i$  is updated as

$$|\tau_i| \mathbf{U}_{\tau_i, n+1}^{\pm, \$} = |\tau_{i,n}^{\pm}| \mathbf{U}_{\tau_i, n}^{\pm} + \sum_j \hat{F}_{ij, n}^{\pm} + \hat{F}_{\tau_i, n}^{\pm}. \quad (4.5)$$

The conservative variables of the flows on the cell  $\tau_i$  is then assigned as

$$\mathbf{U}_{\tau_i, n+1}^{\pm, *} = \begin{cases} 0, & \tau_{i, n+1}^{\pm} = \emptyset, \\ \frac{|\tau_i|}{|\tau_{i, n+1}^{\pm}|} \mathbf{U}_{\tau_i, n+1}^{\pm, \$}, & \tau_{i, n+1}^{\pm} \neq \emptyset. \end{cases} \quad (4.6)$$

Before (4.6) is applied, we declare that the global conservation of the flow variables  $\mathbf{U}_{\tau_i, n+1}^{\pm, \$}$  are preserved without considering the flux on the domain boundary. Precisely, we have

**Lemma 4.1.** *Assuming that*

1. *For every numerical quadrature point  $\mathbf{x}$  in the scheme on  $\Gamma_{\tau, n}^{\text{in}}, \forall \Gamma_{\tau, n}^{\text{in}} \in \Gamma_{h, n}^{\text{in}}, \mathbf{x} + s_{x_i}^{\pm} \mathbf{V}_{\tau, n}^{\pm}$  is not located on  $\partial\Omega$ ;*
2. *The overall numerical flux on  $\partial\Omega$  is vanished.*

Then we have

$$\sum_{\tau_i \in \mathcal{T}} |\tau_i| \mathbf{U}_{\tau_i, n+1}^{\pm, \$} = \sum_{\tau_i \in \mathcal{T}} |\tau_{i,n}^{\pm}| \mathbf{U}_{\tau_i, n}^{\pm} \pm \Delta t_n \sum_{\Gamma_{\tau, n}^{\text{in}} \in \Gamma_{h, n}^{\text{in}}} |\Gamma_{\tau, n}^{\text{in}}| \hat{F}_{\Gamma_{\tau, n}^{\text{in}}}^{\pm}, \quad (4.7)$$

i.e.,

$$\sum_{\tau_i \in \mathcal{T}} |\tau_i| \{ \mathbf{U}_{\tau_i, n+1}^{-, \$} + \mathbf{U}_{\tau_i, n+1}^{+, \$} \} = \sum_{\tau_i \in \mathcal{T}} \{ |\tau_{i,n}^{-}| \mathbf{U}_{\tau_i, n}^{-} + |\tau_{i,n}^{+}| \mathbf{U}_{\tau_i, n}^{+} \}. \quad (4.8)$$

Moreover, the gas density of the flow in both phases satisfies

$$\sum_{\tau_i \in \mathcal{T}} |\tau_i| \rho_{\tau_i, n+1}^{\pm, \$} = \sum_{\tau_i \in \mathcal{T}} |\tau_{i,n}^{\pm}| \rho_{\tau_i, n}^{\pm}. \quad (4.9)$$

*Proof.* By (4.5),

$$\sum_{\tau_i \in \mathcal{T}} |\tau_i| \mathbf{U}_{\tau_i, n+1}^{\pm, \$} = \sum_{\tau_i \in \mathcal{T}} |\tau_{i,n}^{\pm}| \mathbf{U}_{\tau_i, n}^{\pm} + \sum_{\tau_i \in \mathcal{T}} \sum_j \hat{F}_{ij, n}^{\pm} + \sum_{\tau_i \in \mathcal{T}} \hat{F}_{\tau_i, n}^{\pm}.$$

It is clear that

$$\sum_{\tau_i \in \mathcal{T}} \sum_j \hat{F}_{ij,n}^{\pm} = 0,$$

due to the skew-symmetry of the numerical flux  $F(\mathbf{U}_l, \mathbf{U}_r; \mathbf{n})$  and the vanished overall numerical flux on  $\partial\Omega$ .

For a quadrature point  $\mathbf{x} \in \Gamma_{\tau,n}^{\text{in}}, \forall \Gamma_{\tau,n}^{\text{in}} \in \Gamma_{h,n}^{\text{in}}$ , we recall (4.1) that

$$\sum_{k=0}^{K_x} \hat{F}_{\tau,n,\mathbf{x}}^{\pm,k} = \pm \Delta t_n \hat{F}_{\Gamma_{\tau,n}^{\text{in}}}^{\pm},$$

thus by (4.2) and (4.3),

$$\sum_{\tau_i \in \mathcal{T}} \hat{F}_{\tau_i,n}^{\pm} = \pm \sum_{\Gamma_{\tau,n}^{\text{in}} \in \Gamma_{h,n}^{\text{in}}} \Delta t_n |\Gamma_{\tau,n}^{\text{in}}| \hat{F}_{\Gamma_{\tau,n}^{\text{in}}}^{\pm},$$

which provides us that

$$\sum_{\tau_i \in \mathcal{T}} (\hat{F}_{\tau_i,n}^{+} + \hat{F}_{\tau_i,n}^{-}) = 0. \quad (4.10)$$

This gives (4.7) and (4.8) simultaneously. Noting that the first entry of  $\hat{F}_{\Gamma_{\tau,n}^{\text{in}}}^{\pm}$  is always zero, the first entry of  $\sum_{\tau_i \in \mathcal{T}} \hat{F}_{\tau_i,n}^{\pm}$  has to vanish, thus (4.9) follows.  $\square$

We point out that if there may be some cells in the mesh with  $\mathbf{U}_{\tau,n+1}^{\pm,\$} \neq \mathbf{0}$  and  $\tau_{n+1}^{\pm} = \emptyset$ , the assignment in (4.6) will then break down the global conservation of the flow variables, which is originally preserved after  $\mathbf{U}_{\tau,n+1}^{\pm,\$}$  is obtained. Due to (4.6), it is clear that the variation of the conservative variables is quantitatively given as below:

**Corollary 4.1.** *The variation of the conservative variables for either phase is exactly as*

$$\sum_{\tau_i \in \mathcal{T}} |\tau_{i,n+1}^{\pm}| \mathbf{U}_{\tau_i,n+1}^{\pm,*} - \sum_{\tau_i \in \mathcal{T}} |\tau_i| \mathbf{U}_{\tau_i,n}^{\pm,\$} = - \sum_{\tau_i \in \mathcal{T}, \tau_{i,n+1}^{\pm} = \emptyset} |\tau_i| \mathbf{U}_{\tau_i,n+1}^{\pm,\$}.$$

#### 4.4 Post-processing

The scheme using (4.6) to update the solution is equivalent to solving the system on a mesh coupled by the original mesh  $\mathcal{T}$  and the phase interface. Since some of the cells are splitted by the phase interface, the resulted cell fragments may have a size essentially smaller than the typical cell size of the mesh  $\mathcal{T}$ . This is against the CFL constraint and numerical instability is not guaranteed. To remove the numerical instability, we post process the intermediate solution  $\mathbf{U}_{\tau,n}^{\pm,*}$  by the method followed. We first build some cell patches that every cell fragment is included in a patch, and at least one complete cell interior to the phase domain is included in every patch. The conservative flow variables

on every patch are set as the mean values of the corresponding flow variables on the whole patch calculated based on  $\mathbf{U}_{\tau,n}^{\pm,*}$ .

Let us introduce the aggregation algorithm we adopt to build the cell patches at first. The cells with cell fragments are collected in a set

$$\mathcal{S}_n^{\pm} \triangleq \{\tau \in \mathcal{T} : \tau_n^{\pm} \neq \tau \text{ or } \emptyset\}.$$

The cells interior to the phase domain and neighboring to the cell fragment satisfy

$$\mathcal{B}_n^{\pm} \triangleq \left\{ \tau \in \mathcal{T} : \tau_n^{\pm} = \tau \text{ and } \overline{\tau} \cap \overline{\hat{\tau}} \neq \emptyset \text{ for some } \hat{\tau} \in \mathcal{S}_n^{\pm} \right\}.$$

A cell patch is build as a cluster of cells from  $\mathcal{S}_n^{\pm}$  and  $\mathcal{B}_n^{\pm}$ . As the starting point of the aggregation algorithm, the cell patches are initialized as sets with a single cell from  $\mathcal{S}_n^{\pm}$ , denoted as

$$\mathcal{P}_n^{\pm} \triangleq \{\mathcal{P}_{n,i}^{\pm} : \mathcal{P}_{n,i}^{\pm} = \{\tau_i\}, \tau_i \in \mathcal{S}_n^{\pm}\}.$$

The aggregation algorithm is then as

**Algorithm 4.2.**

for every patch  $\mathcal{P}_{n,i}^{\pm} \in \mathcal{P}_n^{\pm}$  do

for every cell  $\tau \in \mathcal{S}_n^{\pm}$  do

if  $\tau$  is neighbored to  $\mathcal{P}_{n,i}^{\pm}$  then

$$\mathcal{P}_{n,i}^{\pm} \rightarrow \mathcal{P}_{n,i}^{\pm} \cup \{\tau\}, \quad \mathcal{S}_n^{\pm} \rightarrow \mathcal{S}_n^{\pm} \setminus \{\tau\},$$

end if

end do

end do

This algorithm stops if no cell fragments are incorporated into the patches  $\mathcal{P}_{n,i}^{\pm} \in \mathcal{P}_n^{\pm}$  any more. With the cell patches built, we set for every cell  $\tau$  in a patch  $\mathcal{P}_{n,i}^{\pm}$ ,

$$\mathbf{u}_{\tau,n}^{\pm} = \sum_{\hat{\tau} \in \mathcal{P}_{n,i}^{\pm}} |\hat{\tau}_n^{\pm}| \mathbf{u}_{\tau,n}^{\pm,*} / \sum_{\hat{\tau} \in \mathcal{P}_{n,i}^{\pm}} |\hat{\tau}_n^{\pm}|, \quad \forall \tau \in \mathcal{P}_{n,i}^{\pm}. \quad (4.11)$$

It is clear we have the following result:

**Lemma 4.2.** *The post-processing based on (4.11) satisfies*

$$\sum_{\tau_i \in \mathcal{T}} |\tau_{i,n}^{\pm}| \mathbf{u}_{\tau,n}^{\pm,*} = \sum_{\tau_i \in \mathcal{T}} |\tau_{i,n}^{\pm}| \mathbf{u}_{\tau,n}^{\pm}.$$

Collecting Lemma 4.1, Corollary 4.1 and Lemma 4.2 from above, the overall algorithm gives us the following quantification on global conservative error:

**Theorem 4.1.** *The numerical solution of two successive time steps satisfies*

$$\sum_{\tau_i \in \mathcal{T}} |\tau_{i,n+1}^\pm| \mathbf{u}_{\tau,n+1}^\pm - \sum_{\tau_i \in \mathcal{T}} |\tau_{i,n}^\pm| \mathbf{u}_{\tau,n}^\pm = \sum_{\tau_i \in \mathcal{T}} \hat{\mathbf{F}}_{\tau_i,n}^\pm - \sum_{\tau_i \in \mathcal{T}, \tau_{i,n+1}^\pm = \emptyset} |\tau_i| \mathbf{u}_{\tau_i,n+1}^{\pm,\$},$$

and

$$\begin{aligned} & \sum_{\tau_i \in \mathcal{T}} \{ |\tau_{i,n+1}^+| \mathbf{u}_{\tau,n+1}^+ + |\tau_{i,n+1}^-| \mathbf{u}_{\tau,n+1}^- \} - \sum_{\tau_i \in \mathcal{T}} \{ |\tau_{i,n}^+| \mathbf{u}_{\tau,n}^+ + |\tau_{i,n}^-| \mathbf{u}_{\tau,n}^- \} \\ &= - \sum_{\iota \in \{+, -\}} \sum_{\tau_i \in \mathcal{T}, \tau_{i,n+1}^\iota = \emptyset} |\tau_i| \mathbf{u}_{\tau_i,n+1}^{\iota,\$}. \end{aligned}$$

*Proof.* The first equality is a direct inference of Lemma 4.1, Corollary 4.1 and Lemma 4.2. The second equality is given by the summation of the first equality for both phase and (4.10).  $\square$

The post processing as (4.11) actually makes the numerical flux between the cells in the same patch cancel each other. Thus the updation of (4.6) is revised to calculate the numerical flux on the boundary of the cell patches instead of on the boundary of every cell. Since there is at least one complete cell in every patch, the CFL constraint is thus satisfied. This makes the whole numerical scheme to be stabilized.

**Remark 4.1.** If a small patch of the gas is isolated from the bulk of the corresponding phase, it is possible that the whole patch of gas can not cover even one single cell in the mesh. As the result, the set  $\mathcal{S}_n^\pm$  is not empty after the Algorithm 4.2 is ended. In such case, we incorporate all the remaining cells in  $\mathcal{S}_n^\pm$  connected to each other to be a single patch. We refer such cell patches without complete cell at all as "islet".

**Remark 4.2.** If an islet is so small that its volume is less than a prescribed tolerance, we directly assign the flow variables in the islet to be a default state. The default state is with very low pressure that the islet is gradually shrinking and eventually automatically disappears. This is very effective to eliminate too complex phase interface geometry due to these small islets thus the both the overall computational cost and the quality of the numerical solution are under control. As a negative side effect, the conservation of the flow variables will be spoiled again by such an artificial technique.

## 5 Numerical results

Let us present some numerical examples to validate our numerical method. These numerical examples include some Riemann problems and some shock impact problems. Our simulations are carried out on  $h$ -type adaptive meshes, while the detailed techniques are not presented here.



## 5.1 Riemann problem

### 5.1.1 One-phase Riemann problem

In the first example, we study a simple one-phase problem, which is called Sod shock tube problem, where a standard Eulerian scheme also works well with no oscillation. The numerical results are compared with the exact solutions.

Let the domain  $\Omega = (0.0, 1.0) \times (0.0, 0.5)$ . The initial value is

$$[\rho, u, v, p, \gamma] = \begin{cases} [1.0, 0, 0, 1.0, 1.4], & x < 0.5, \\ [0.125, 0, 0, 0.1, 1.4], & x > 0.5. \end{cases}$$

The boundary values for both phases are appointed that the problem is essentially an one dimensional problem excepted for the tangential slip in the  $y$  direction for each phase. Though there is actually only one fluid, we take it as a two-phase problem by artificially embedding an interface at  $x = 0.5$  when  $t = 0$ . We carry out the simulation to a final time of 0.25s, and adaptive mesh refinement is adopted to capture the interface and shock front. Fig. 1 shows the numerical results for respective density, velocity, pressure and internal energy obtained, for comparison to the exact solutions. In these figures we see that the numerical results behave in perfect agreement with the exact solutions. Fig. 2 shows the location and shape of the interface at different times, which shows that both the interface and the shock front are resolved correctly.

### 5.1.2 Two-phase Riemann problem

In this example, we study a two-phase problem, which has the same initial values as the first example except for the value of  $\gamma$  in phase 1. Similarly, let the domain  $\Omega = (0.0, 1.0) \times (0.0, 0.5)$ . The initial value is

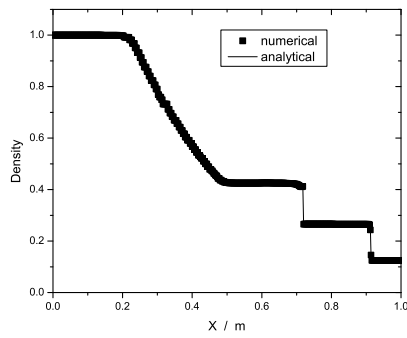
$$[\rho, u, v, p, \gamma] = \begin{cases} [1.0, 0, 0, 1.0, 1.2], & x < 0.5, \\ [0.125, 0, 0, 0.1, 1.4], & x > 0.5. \end{cases}$$

The boundary conditions for both phases are the same as the first example. The simulation is ended at a final time of 0.152s. Fig. 3 shows the numerical results obtained for comparison to the exact solutions, where we see that there is no non-physical oscillation in the vicinity of the interface. Fig. 4 shows the location and shape of the interface at different times, in which the interface can be kept approximately as a straight line during its evolving.

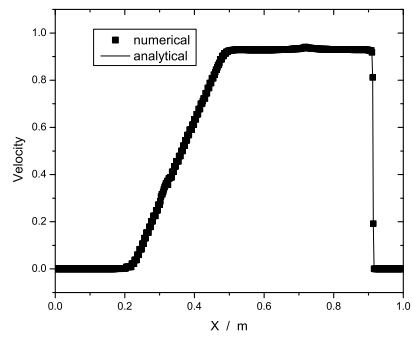
### 5.1.3 Strong shock two-phase Riemann problem

In this example, we explore a strong shock tube problem, where phase 0 and phase 1 across the interface have quite big density ratio  $\rho_l / \rho_r = 1000$  and pressure ratio  $p_l / p_r = 1000$ . We still let the domain  $\Omega = (0.0, 1.0) \times (0.0, 0.5)$ . The initial value is

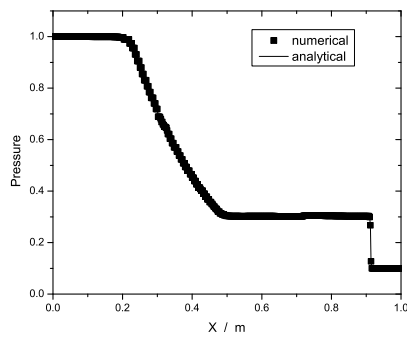
$$[\rho, u, v, p, \gamma] = \begin{cases} [1000, 0, 0, 10^8, 1.2], & x < 0.5, \\ [1, 0, 0, 10^5, 1.4], & x > 0.5. \end{cases}$$



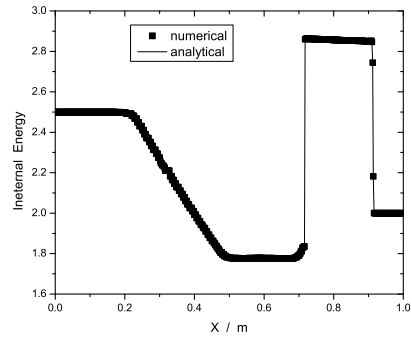
(a) Density



(b) Velocity



(c) Pressure



(d) Internal energy

Figure 1: Solution at time=0.25s.

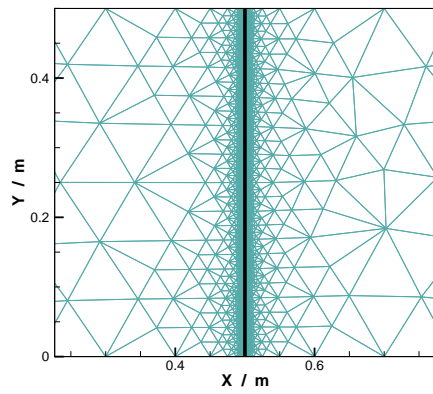
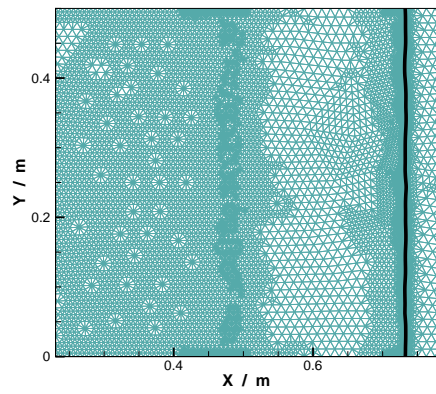
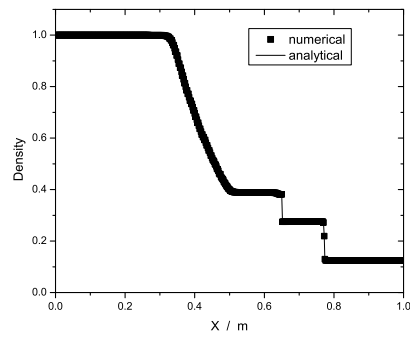
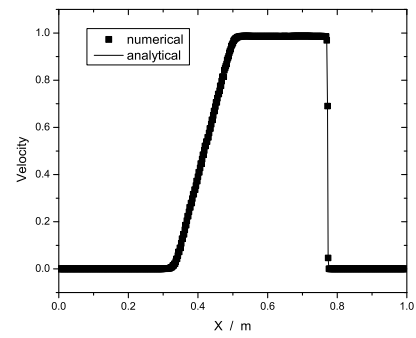
(a)  $t=0$ (b)  $t=0.25s$ 

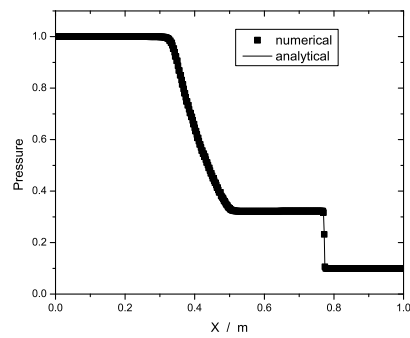
Figure 2: Phase interface at different times.



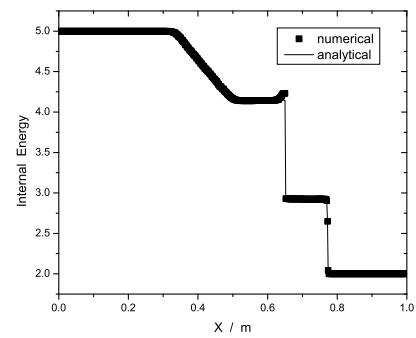
(a) Density



(b) Velocity



(c) Pressure



(d) Internal energy

Figure 3: Solution at time=0.152s.

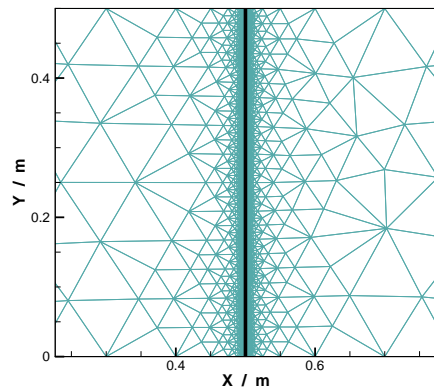
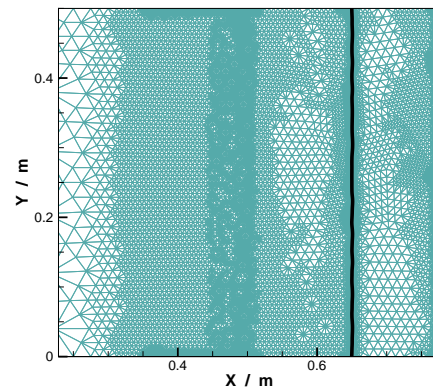
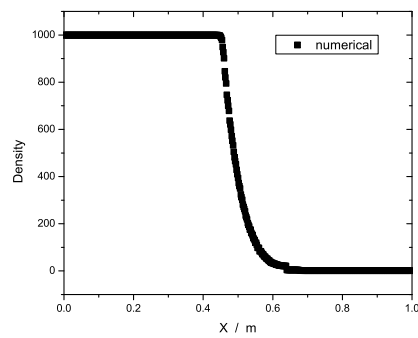
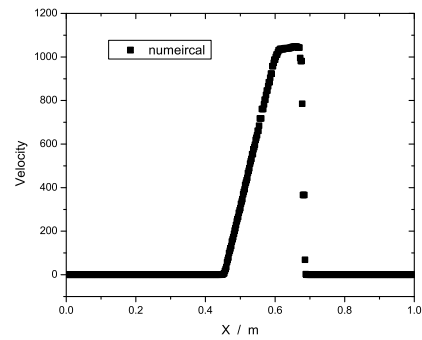
(a)  $t=0$ (b)  $t=0.152s$ 

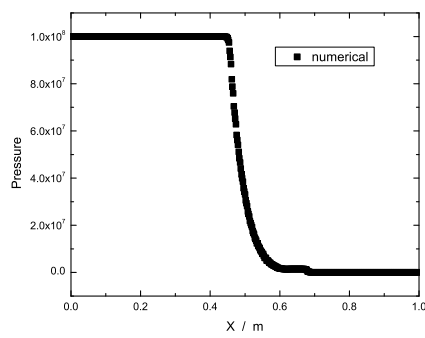
Figure 4: Phase interface at different times.



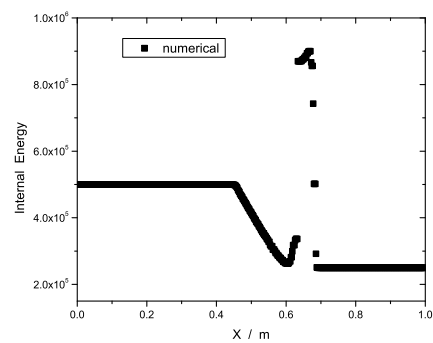
(a) Density



(b) Velocity



(c) Pressure



(d) Internal energy

Figure 5: Solution at time=0.00013s.

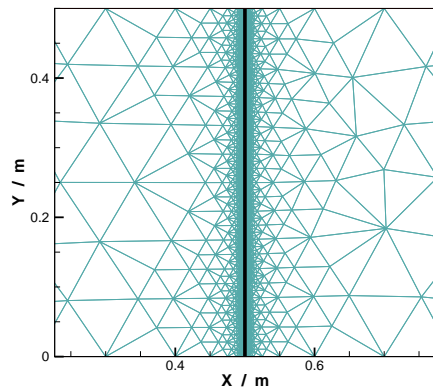
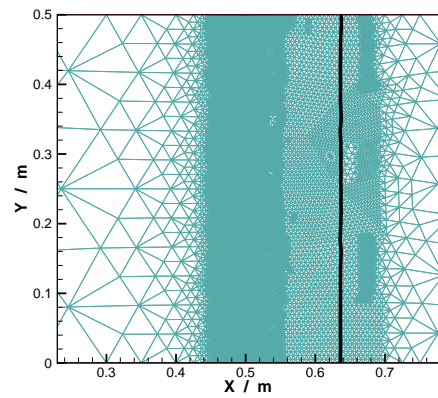
(a)  $t=0$ (b)  $t=0.00013s$ 

Figure 6: Phase interface at different times.

The boundary values for both phases are the same as the first example again. The simulation is ended at a final time of 0.00013s. Fig. 5 shows the numerical results obtained, in which we see that there is also no non-physical oscillation around the interface. Fig. 6 shows the location and shape of the interface at different times, which shows that the interface is kept quite well.

## 5.2 Planar shock impact

Let the domain be the two-dimensional plane as  $\Omega = \{(x, y) : x \in (-10, 10), y \in (-10, 10)\}$ . The initial value is

$$[\rho, u, v, p, \gamma] = \begin{cases} [100, 0, 0, 10^{10}, 1.2], & \sqrt{x^2 + y^2} < 0.3, \\ [1.29, 0, 0, 10^5, 1.4], & \sqrt{x^2 + y^2} > 0.3. \end{cases}$$

The boundary values for both phases are set as outflow boundary conditions. Fig. 7 shows the field pressure contours obtained at different times, where we see that the shock wave propagates as a finite speed into the around gas. Fig. 8 shows the location and shape of the interface at different times, which shows that interface is approximately kept as a circle, in agreement with the corresponding physical process.

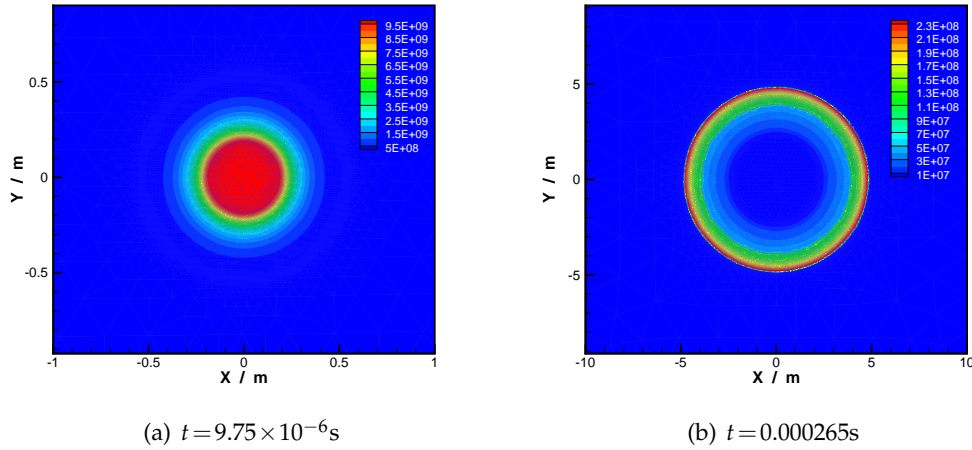


Figure 7: Pressure contours at different times.

## 5.3 Spherical shock impact

Let the domain to be the cylinder as  $\Omega = \{(r, z) : r \in (0, 5000), z \in (0, 1.0 \times 10^4)\}$ . The initial value is

$$[\rho, u, v, p, \gamma] = \begin{cases} [618.935, 0, 0, 6.314 \times 10^{12}, 1.2], & \sqrt{r^2 + (z - 5000)^2} < 0.3, \\ [1.29, 0, 0, 10^5, 1.4], & \sqrt{r^2 + (z - 5000)^2} > 0.3. \end{cases}$$

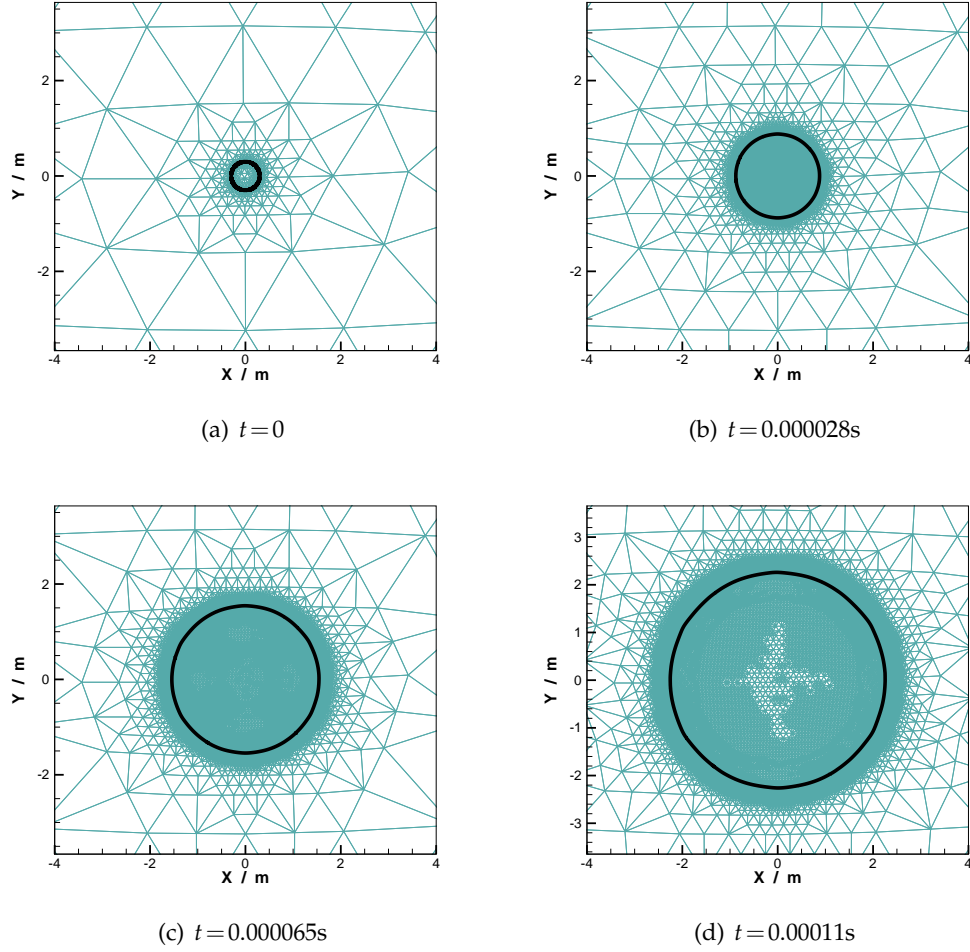


Figure 8: Phase interface at different times.

The Euler equations for this configuration is reformulated into a cylindrical formation as

$$\frac{\partial \mathbf{U}}{\partial t} + \frac{\partial \mathbf{F}(\mathbf{U})}{\partial r} + \frac{\partial \mathbf{G}(\mathbf{U})}{\partial z} = \mathbf{S}(\mathbf{U}),$$

where

$$\mathbf{U} = \begin{bmatrix} r\rho \\ r\rho u \\ r\rho v \\ rE \end{bmatrix}, \quad \mathbf{F}(\mathbf{U}) = \begin{bmatrix} r\rho u \\ r(\rho u^2 + p) \\ r\rho uv \\ r(E+p)u \end{bmatrix}, \quad \mathbf{G}(\mathbf{U}) = \begin{bmatrix} r\rho v \\ r\rho uv \\ r(\rho v^2 + p) \\ r(E+p)v \end{bmatrix}, \quad \mathbf{S}(\mathbf{U}) = \begin{bmatrix} 0 \\ p \\ 0 \\ 0 \end{bmatrix},$$

and here  $u$  is the radial velocity. The source term  $\mathbf{S}(\mathbf{U})$  is due to the cylindrical coordinate transformation.

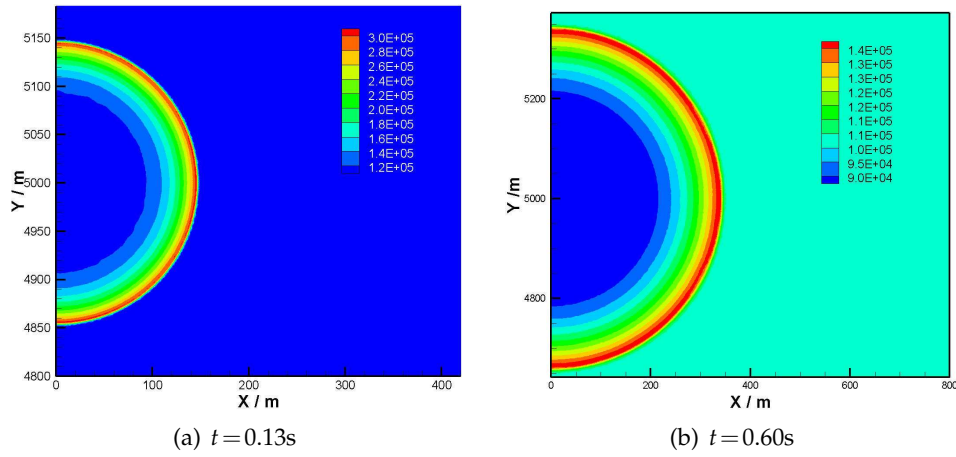


Figure 9: Pressure contours at different times.

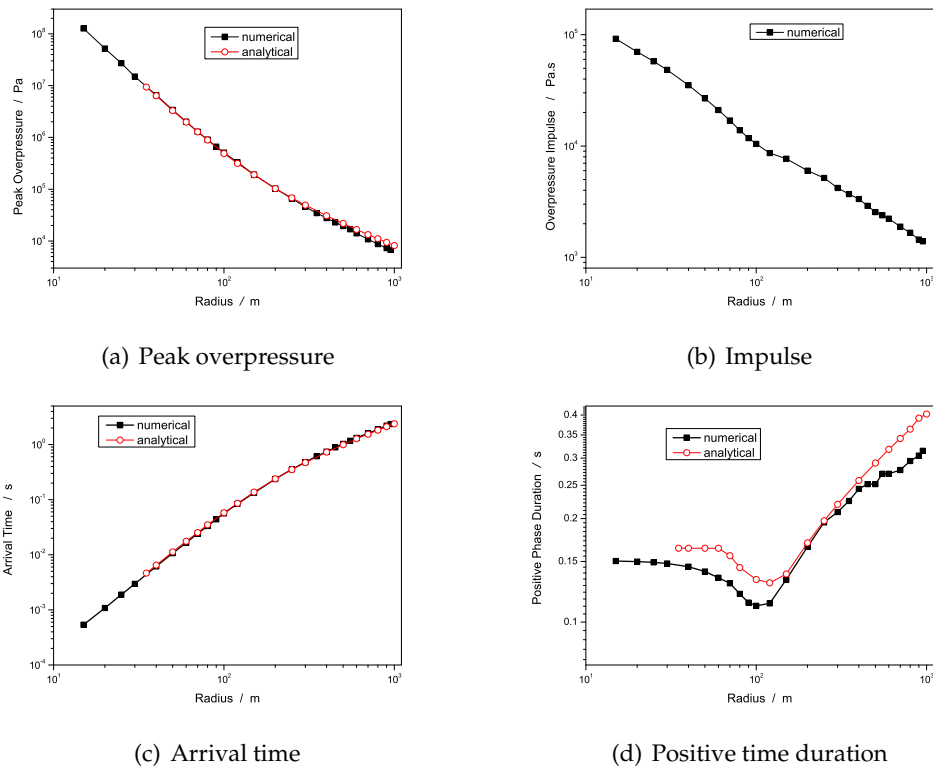


Figure 10: Shock wave parameters in distance from the center.

This example is actually used to simulate the blast waves from one kiloton nuclear charge. Fig. 9 shows the field pressure contours obtained at different times, where one

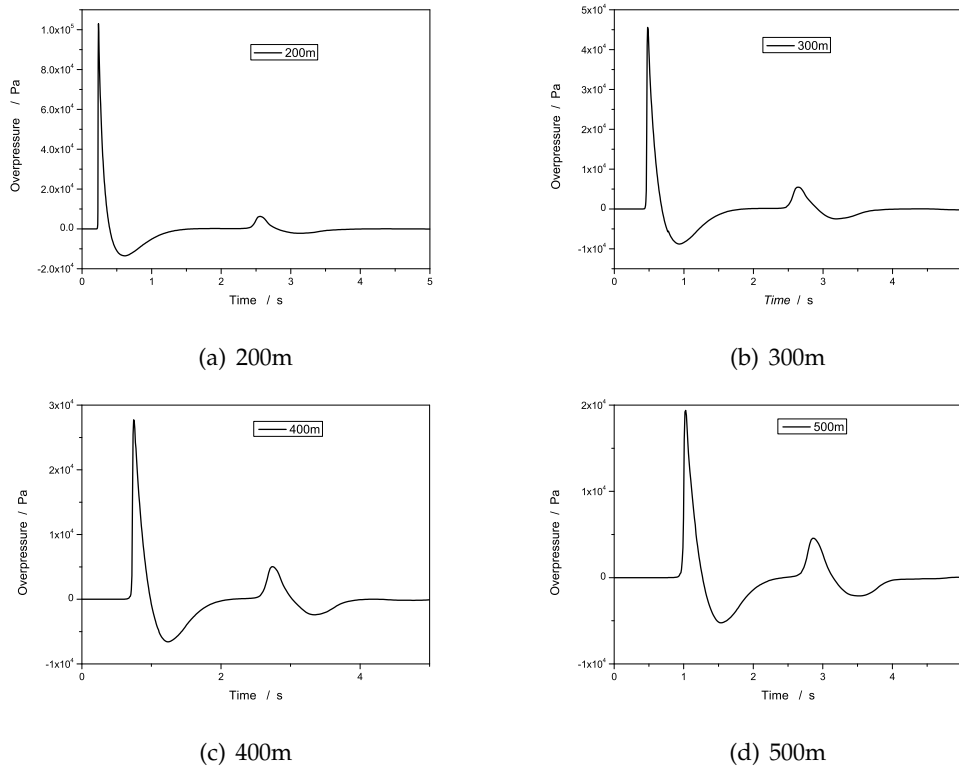


Figure 11: Pressure in time at fixed points.

may see the propagation and decay of the shock front, qualitatively in agreement with the corresponding physical process. Fig. 10 shows the calculated blast wave parameters at different radii, compared with the "point explosion solution" [10]. Fig. 11 shows the curves of overpressure in time at some fixed radii away from the burst point. In these figures, it is clear that when a shock wave arrives, the pressure increases rapidly to a peak value, then reduces to a low pressure smaller than its initial value. When the secondary shock wave arrives, the pressure increases again but comparatively slowly. After the secondary shock wave propagates away, the pressure eventually goes back to its initial value.

## 6 Conclusions

We developed a numerical method to simulate two-phase compressible flows on Eulerian grids. The scheme is a combination of the front tracking method and the levelset method. The implementation of the scheme is straightforward and some preliminary numerical examples validate our method.



## Acknowledgements

We thank the anonymous referee's help to revise the manuscript. This research was supported in part by NSF in China (No. 11325102, 91330205).

## References

- [1] J. U. BRACKBILL, D. B. KOTHE, AND H. M. RUPPEL, *FLIP: a low-dissipation, particle-in-cell method for fluid flow*, Comput. Phys. Commun., 48(1) 91988), pp. 25–38.
- [2] YANA DI, RUO LI, TAO TANG, AND PINGWEN ZHANG, *Level set calculations for incompressible two-phase flows on a dynamically adaptive grid*, J. Sci. Comput., 31(1-2) (2007), pp. 75–98.
- [3] DOUGLAS ENRIGHT, RONALD FEDKIW, JOEL FERZIGER, AND IAN MITCHELL, *A hybrid particle level set method for improved interface capturing*, J. Comput. Phys., 183(1) (2002), pp. 83–116.
- [4] SIMONE E HIEBER AND PETROS KOUMOUTSAKOS, *A Lagrangian particle level set method*, J. Comput. Phys., 210(1) (2005), pp. 342–367.
- [5] SEIICHI KOSHIZUKA, ATSUSHI NOBE, AND YOSHIKI OKA, *Numerical analysis of breaking waves using the moving particle semi-implicit method*, Int. J. Numer. Methods Fluids, 26(7) (1998), pp. 751–769.
- [6] PETROS KOUMOUTSAKOS, *Multiscale flow simulations using particles*, Ann. Rev. Fluid Mech., 37 (2005), pp. 457–487.
- [7] JOE J. MONAGHAN, *Smoothed particle hydrodynamics*, Reports Progress Phys., 68(8) (2005), pp. 1703.
- [8] WILLIAM F. NOH AND PAUL WOODWARD, *SLIC (Simple Line Interface Calculation)*. In Proceedings of the Fifth International Conference on Numerical Methods in Fluid Dynamics June 28–July 2, 1976, Twente University, Enschede, pp. 330–340, Springer, 1976.
- [9] STANLEY OSHER AND RONALD P. FEDKIW, *Level set methods: an overview and some recent results*, J. Comput. Phys., 169(2) (2001), pp. 463–502.
- [10] DENGJIANG QIAO, *An Introduction to Nuclear Explosion Physics*, National Defence Industry Press (in Chinese), 2003.
- [11] WILLIAM J RIDER AND DOUGLAS B KOTHE, *Stretching and tearing interface tracking methods*, in AIAA Computational Fluid Dynamics Conference, 12th, and Open Forum, San Diego, CA, pp. 806–816, 1995.
- [12] I. F. SBALZARINI, JENS HONORE WALTHER, M. BERGDORF, S. E. HIEBER, E. M. KOTSALIS, AND P. KOUMOUTSAKOS, *PPM—a highly efficient parallel particle–mesh library for the simulation of continuum systems*, J. Comput. Phys., 215(2) (2006), pp. 566–588.
- [13] RUBEN SCARDOVELLI AND STÉPHANE ZALESKI, *Direct numerical simulation of free-surface and interfacial flow*, Ann. Rev. Fluid Mech., 31(1) (1999), pp. 567–603.
- [14] JAMES A. SETHIAN, *Evolution, implementation, and application of level set and fast marching methods for advancing fronts*, J. Comput. Phys., 169(2) (2001), pp. 503–555.
- [15] MARK SUSSMAN, *A second order coupled level set and volume-of-fluid method for computing growth and collapse of vapor bubbles*, J. Comput. Phys., 187(1) (2003), pp. 110–136.
- [16] MARK SUSSMAN, PETER SMEREKA, AND STANLEY OSHER, *A level set approach for computing solutions to incompressible two-phase flow*, J. Comput. Phys., 114(1) (1994), pp. 146–159.
- [17] GRÉTAR TRYGGVASON, BERNARD BUNNER, ASGSGHAR ESMAEELI, DAMIR JURIC, N. AL.-RAWAHI, W. TAUBER, J. HAN, S. NAS, AND Y. J. JAN, *a front-tracking method for the computations of multiphase flow*, J. Comput. Phys., 169(2) (2001), pp. 708–759.

- [18] S. O. UNVERDI AND G. TRYGGVASON, *A front-tracking method for viscous, incompressible, multi-fluid flows*, J. Comput. Phys., 100(1) (1992), pp. 25–37.
- [19] JENS HONORE WALTHER, T. WERDER, R. L. JAFFE, AND P. KOUMOUTSAKOS, *Hydrodynamic properties of carbon nanotubes*, Phys. Rev. E, 69(6) (2004), pp. 062201.
- [20] HAN YOUNG YOON, SEIICHI KOSHIZUKA, AND YOSHIAKI OKA, *Direct calculation of bubble growth, departure, and rise in nucleate pool boiling*, Int. J. Multiphase Flow, 27(2) (2001), pp. 277–298.